Sol–gel-immobilised terbium complexes for luminescent sensing of dissolved oxygen by analysis of emission decay†

Stephanie Blair, Ritu Kataky and David Parker*

Department of Chemistry, University of Durham, South Road, Durham, UK DH1 3LE

Received (in London, UK) 21st November 2001, Accepted 5th March 2002
First published as an Advance Article on the web 18th April 2002

Cationic terbium complexes bearing an *N*-methylphenanthridinium chromophore have been incorporated in sol–gel thin films and their response characteristics analysed with respect to variations in dissolved oxygen concentration. Analysis of the emission lifetime decay curves (547 nm) has allowed a linear calibration model to be defined over an oxygen concentration range from zero to 0.5 mM (H_2O, 295 K).

The ability to measure and monitor the level of dissolved oxygen in water is important in a variety of biological, environmental and industrial applications.[1] For example, in river waters, hypoxia can alter the behaviour of fish when the oxygen concentration falls below 0.1 mM, while concentrations of less than 35 μM will usually cause death.[2] The biochemical breakdown of sewage is undertaken by bacteria working in aerobic conditions, thus dissolved oxygen monitoring is necessary in waste treatment plants as an inadequate supply of oxygen can enhance the activity of anaerobic sulfate-reducing bacteria, producing hydrogen sulfide. Knowledge of oxygen gradients in complex biological samples is of importance in understanding many biological processes, including aerobic energy metabolism. This creates a need for sensitive and selective methods of detection, operating in real-time and which are non-invasive. Optical sensors offer much scope in this respect[3,4] as they are not easily poisoned, respond quickly and do not consume O_2—in contrast to conventional electrochemical methods. They are also amenable to minituarisation, either as fibre-optic optodes[5] or in stabilised liposomes or nanoparticles.[4,6]

In most cases, oxygen sensitivity in the critical 'indicator' molecule or complex is based on the quenching of luminescence of a conjugated chromophore or metal complex. Examples include polycyclic aromatic hydrocarbons (pyrenes, perylenes, phenanthrene),[7,8] often immobilised in oxygen-permeable polymers such as polystyrene or silicon rubber, and diketones such as camphorquinone encapsulated in PVC and silica gel.[9] However, luminescent Ru(II) diimine complexes predominate among optical oxygen sensors,[3,9,10] exhibiting high quantum yields and relatively long luminescent lifetimes. Many examples of oxygen-sensitive metalloporphyrins have also been reported,[9,11–13] with complexes of Pd and Pt exhibiting emission lifetimes in the millisecond range, sensitive to pO_2.

In the last few years, a number of reports have appeared describing the sensitivity of the emission intensity and lifetime of certain lanthanide complexes to oxygen.[14–17] This dependence does not normally reflect any quenching of the lanthanide excited state, but relates to the quenching of the intermediate triplet state of the antenna chromophore in examples of sensitised luminescence. This sensitivity to pO_2 arises when the rate of forward intramolecular energy transfer from the antenna triplet to the accepting Ln^{3+} ion is competitive with bimolecular quenching by oxygen, *i.e.* when k_{ET} is comparable to $k_q[O_2]$. In particular, more pronounced oxygen sensitivity has been reported when there is a finite rate of reverse energy transfer from the excited Ln^{3+} state repopulating the triplet state of the chromophore. For this thermally activated process to be significant at ambient temperature, the energy gap between the two states usually needs to be less than 1500 cm^{-1}. For this reason, most examples in this class have involved Tb complexes, as its $^5D_4$ excited state, lying at 20,400 cm^{-1}, is closer to the energy of the triplet states of a wide range of aromatic chromophores. Recently, a series of near-IR luminescent complexes (Nd, Er, Yb) has been described, in which fluorescein, eosin or a metalloporphyrin acts as the sensitising chromophore.[18–20] Here, it is the slowness of the intramolecular energy transfer step which renders the emission intensity and lifetime dependent on dissolved oxygen concentration.

The only published examples of oxygen sensing with lanthanide complexes in thin films are due to Amao *et al.*[21–23] Europium β-diketonate complexes bearing a phenanthroline chromophore have been incorporated into modified polystyrene films and exhibit near linear Stern–Volmer plots with modest sensitivity to oxygen in the gas phase. Terbium analogues have been used to dope alumina films in gaseous analyses and showed curved Stern–Volmer plots, apparently characteristic of multi-site quenching.

In seeking to immobilise oxygen-sensitive terbium complexes to allow analysis of dissolved oxygen, we were attracted by the utility of sol–gel thin films.[24] Sol–gel glass is an optically transparent, porous and homogeneous material, favouring its use as a sensor matrix. Moreover, it is more chemically inert and photostable than organic polymers and the controlled preparation of thin films of defined porosity is relatively well understood. Sol–gel-encapsulated ruthenium complexes have been defined for dissolved oxygen assay by MacCraith and co-workers,[25,26] but the examples reported herein define the first lanthanide complexes immobilised for this purpose. The terbium complexes chosen, $[Tb{\cdot}\mathbf{1}]^{+}$ [17] and $[Tb{\cdot}\mathbf{2}]^{4+}$ [26] (Scheme 1), are very stable with respect to acid-mediated dissociation. This is a requirement as the conditions for sol–gel formation and encapsulation of the complex are strongly acidic. Each complex possesses an *N*-methylphenanthridinium chromophore, with an extinction coefficient of 5000 M^{-1} cm^{-1} at 370 nm.[27,28] The energy gap between the $^5D_4$ Tb^{3+} excited

† Electronic supplementary information (ESI) available: examples of the analysis of the emission decay data for calibration purposes and examples of data sets and their treatment at different delay times. See http://www.rsc.org/suppdata/nj/b1/b110743g/

 DOI: 10.1039/b110743g

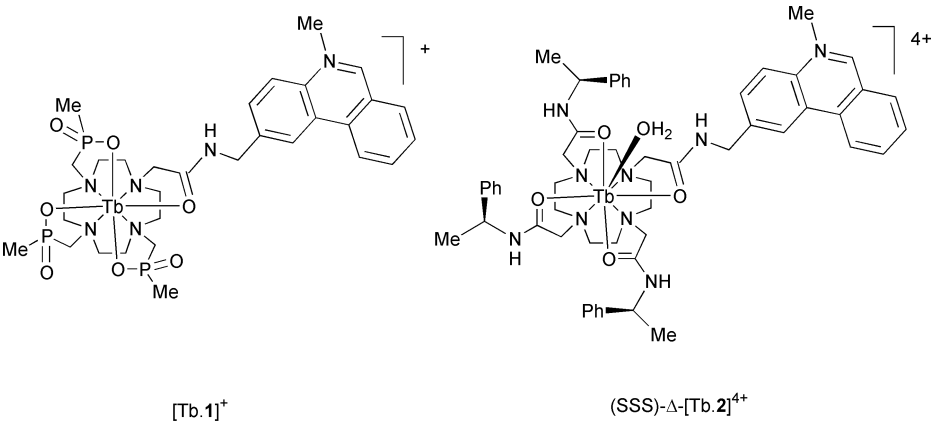

[Tb.**1**]$^{+}$ (SSS)-Δ-[Tb.**2**]$^{4+}$

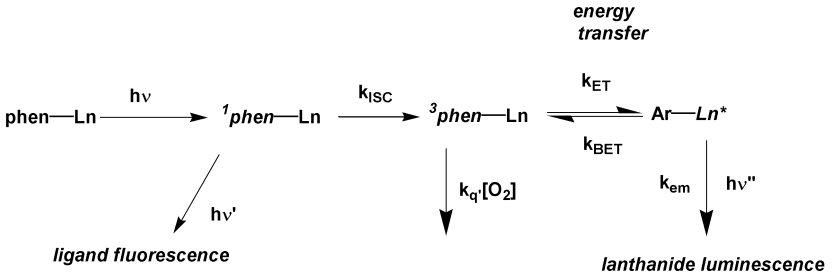

Scheme 1

state and the aryl triplet is only 900 cm^{-1}, leading to the observed sensitivity to dissolved oxygen.[17]

Experimental

Luminescence measurements were performed on an Instruments SA Fluorolog 3–11 equipped with an SPX 1934D3 phosphorimeter. Corrected spectra were obtained to compensate for the wavelength-dependent response of the instrument. Excitation and emission wavelengths were selected using single grating monochromators and the intensity was measured with the aid of a Hamamatsu R928 photomultiplier tube. Spectral artefacts (second order transmission, scattered excitation light) were avoided by using appropriate cut-off filters. Details of the flow cell used have been reported recently.[29] It uses internal reflection to capture and guide the emitted luminescence towards the detector and light emission is observed at 90° to the centrally illuminated film. Emission slits were typically 2 nm, allowing good spectral resolution without compromising signal intensity.

Film preparation

Sol–gel films were produced by adding acidified water (0.1 mol dm^{-3} HCl) to a solution of ethanol and ethyltriethoxysilane (ETEOS). The molar ratios of the precursors used to fabricate the films were based on sol–gel film preparations for dissolved oxygen sensing described by MacCraith *et al.*[30] The molar ratio of water to ETEOS (R) was either 2 or 4. All films were prepared with an ethanol to ETEOS molar ratio of 8. Following stirring of the sol at 295 K for 40 min, the relevant Tb complex was added (5 mmol dm^{-3}). The sol was then aged at 295 K for a fixed period. During this ageing period, the sol was stirred. Thin films were cast by dropping 100 μL of the sol solution onto one side of a rotating quartz disc. Prior to spin-coating, the quartz substrates were placed overnight in conc. HNO_3 to activate the surface of the quartz, and then cleaned sequentially using water and ethanol. All films were spun at 2400 rpm using a Cammex Precima PRS14E spin-coater. After coating, all films were left in ambient laboratory conditions to stabilise for periods up to 28 days prior to analysis in order to allow structural changes within the sol–gel matrix to evolve.[31] Membrane compositions are summarized in Table 1.

Dissolved oxygen measurements

Aqueous dissolved oxygen measurements were made using a Jenway model 9150 dissolved oxygen meter. Prior to usage, a two-point calibration was performed, in which the probe was immersed in a 0.16 mol dm^{-3} solution of sodium sulfite to obtain a 0% dissolved oxygen reading. The probe was then rinsed with clean water and placed approximately 1 cm into a beaker of clean water to obtain a 100% dissolved oxygen reading. The experimental set-up used for dissolved oxygen sensing is shown in Fig. 1. Sol–gel films incorporated into the flow-cell were exposed to water (flow rate 4 ml min^{-1}) of a defined dissolved oxygen concentration. Using a peristaltic pump, the water was passed continuously round a closed flow

Table 1 Composition, ageing and stabilisation time of sol–gel films for dissolved oxygen sensing

Complex immobilised in sol–gel film	ETEOS:H_2O	ETEOS:EtOH	Ageing/h	Stabilisation/days	Concentration of complex/mmol dm^{-3}
[Tb·**1**]$^{+}$	1:2	1:8	4	126	5
[Tb·**2**]$^{4+}$	1:2	1:8	26	75	5
[Tb·**2**]$^{4+}$	1:4	1:8	26	75	5

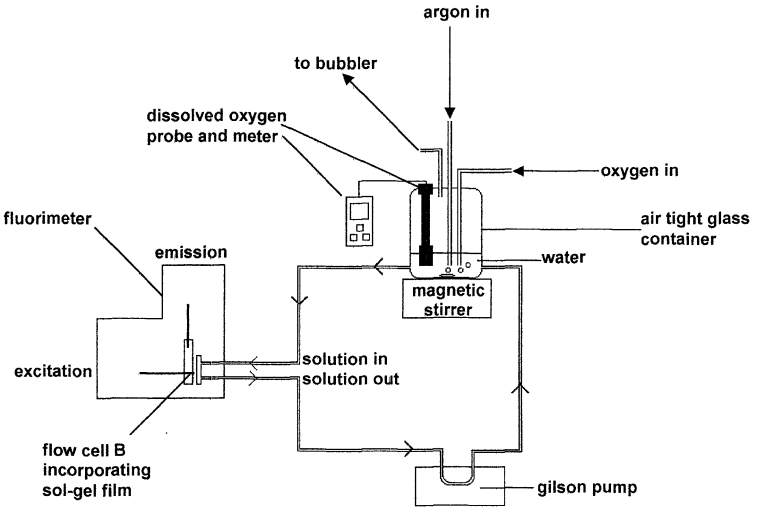

Fig. 1 Schematic representation of the flow apparatus used for dissolved oxygen measurements using sol–gel films.

system *via* a mixing chamber, where the water was purged with argon and oxygen. Water and gases were stirred vigorously using a magnetic stirrer. Different dissolved oxygen concentrations were produced using fine needle valves to control the gas flow rate from the gas regulators to the mixing vessel. The dissolved oxygen sensing probe was immersed in the water inside the chamber to monitor the dissolved oxygen concentration which was displayed on the portable display meter attached to the probe.

Spectra were recorded when measuring the metal-based emission after the concentration of dissolved oxygen in the water had stabilised (as indicated by a stable reading on the portable display attached to the dissolved oxygen probe), and then at intervals typically of 10 and 15 min, to ensure the signal was stable. Excitation and emission wavelengths corresponding to $\lambda_{ex} = 330$ nm and $\lambda_{em} = 547$ nm were used. Excitation slits were set at 7 nm bandpass for the sol–gel film incorporating $[Tb\cdot\mathbf{1}]^{+}$, and 10 nm bandpass for the sol–gel films incorporating $[Tb\cdot\mathbf{2}]^{4+}$. The emission slits were 2 and 3 nm bandpass respectively. All spectra were recorded using increments of 0.5 nm and 0.25 s for the integration setting.

Intensity decay data were recorded following the excitation of the sol–gel films by a short flash of light ($\lambda = 330$ nm). The integrated intensity of emitted light ($\lambda = 547$ nm) was recorded following an initial delay of 0.01 ms, and then at delay times of t_d ($t_d = 0.05$ ms for the sol–gel films incorporating $[Tb\cdot\mathbf{1}]^{3+}$ or $[Tb\cdot\mathbf{2}]^{4+}$, where $R = 2$, $t_d = 0.1$ ms for the sol–gel film incorporating $[Tb\cdot\mathbf{2}]^{4+}$ where $R = 4$). The sampling window was set at 15 ms. The time between flashes was set to 40 ms and the total number of flashes was up to 500.

Excitation and emission slits were set at 20 and 10 nm bandpass, respectively, for the film incorporating complex $[Tb\cdot\mathbf{1}]^{+}$ and 25 and 20 nm bandpass, respectively, for the films incorporating complex $[Tb\cdot\mathbf{2}]^{4+}$. Measurements were recorded when the concentration of dissolved oxygen in the water had stabilised (as indicated by a stable reading on the portable display attached to the dissolved oxygen probe). All measurements were performed at 295 K. The analysis of the emission decay data for calibration purposes is described in the text and examples are given in the ESI.

Results and discussion

Quenching may be described by the Stern–Volmer equation. In homogeneous media, each luminescent species experiences the same average microenvironment, often resulting in 'single component' exponential decay of the emission intensity. The intensity and lifetime forms of the Stern–Volmer equation are represented by eqn. (1–3),[32]

$$\frac{\tau_O}{\tau} = 1 + K_{SV}[O_2] \quad (1)$$

$$K_{SV} = k_2\tau_O \quad (2)$$

$$\frac{I_O}{I} = 1 + (K_{SV} + K_{eq})[O_2] + K_{eq}K_{SV}[O_2]^2 \quad (3)$$

where τ and τ_O are the lifetimes in the presence and absence of O_2, respectively, K_{SV} is the Stern–Volmer constant, k_2 a bimolecular quenching constant and K_{eq} an association constant describing the binding of the O_2 quencher to the luminescent species. The efficacy of the quencher or the accessibility of the chromophore to the quencher is given by $k_2{:}k_2 = \alpha D$, where α is the solubility coefficient and D the diffusion coefficient of the O_2 in the environment of the chromophore. Eqn. (3) considers the possibility of both dynamic and static (formation of a non-luminescent complex) quenching.

The emission of the terbium complexes $[Tb\cdot\mathbf{1}]^{+}$ and $[Tb\cdot\mathbf{2}]^{4+}$ has been described in aqueous solution,[17] and linear Stern–Volmer plots were observed (Table 2). In each case, the behaviour was independent of pH over the range 2 to 9. The cationic terbium complexes were incorporated in thin-film sol–gel matrices as described in the Experimental section, and their response characteristics assessed as a function of dissolved oxygen concentration. In particular, the emission decay profiles ($\lambda_{em} = 547$ nm) were monitored. For cases where quenching occurs in a solid matrix, such as a sol–gel, the microheterogeneity of complex distribution results in non-linear intensity Stern–Volmer plots.[30] Luminescent lifetime decays also often display complex profiles and analyses based on eqn. (1–3) are therefore inappropriate. In order to analyse the situation with the terbium complexes discussed here, the following photophysical model was adopted, (Scheme 1). The kinetic scheme reveals that the dependence of the terbium

Table 2 Stern–Volmer constants and lifetimes in aqueous solution for $[Tb\cdot\mathbf{1}]^{+}$ and $[Tb\cdot\mathbf{2}]^{4+}$

Complex[a]	K_{SV}^{-1} [b]/Torr	τ (no O_2)[c]/ms	τ (aerated)/ms
$[Tb\cdot\mathbf{1}]^{+}$	45	0.83	0.10
$[Tb\cdot\mathbf{2}]^{4+}$	58	0.94	0.09

[a] 293 K; $\lambda_{exc} = 370$ nm, $\lambda_{em} = 545$ nm; $I = 0.1$ M NMe_4ClO_4. [b] Measurements made in the range 0 to 0.3 mM O_2. [c] At 293 K and 1 atm, the solubility of O_2 in water is 8.7 mg L^{-1}, *i.e.* 0.27 mM.

emission decay rate on O_2 is intrinsically complex, being an example of two coupled decay processes for which mathematical solutions have been defined.[33] Attempts were made to fit the experimental decay profiles to kinetic schemes of varying complexity. It was found that a reliable method of treating the data could be found by making the assumption that the rate of back energy transfer is much less than k_{em}, where k_{em} is the rate constant defining radiative decay of the lanthanide excited state. Under these conditions, the fraction of the triplet phenanthridinium state quenched by energy transfer to the $^5D_4$ emissive level of Tb^{3+} is described by eqn. (4):

$$\frac{k_{ET}}{(k_{ET} + k_Q[O_2]^n)} = \frac{I_t}{I_t^0} \quad (4)$$

where k_{ET} is the rate of forward energy transfer process, k_Q is the rate constant for the biomolecular rate quenching process, I_t the intensity at time t and I^0 denotes intensity in the absence of quencher.

If the ratio I_t/I_t^0 is replaced by R, eqn. (4) may be rearranged to give eqn. (5).

$$k_{ET} = R(k_{ET} + k_Q[O_2]^n) \quad (5)$$

Further rearrangements give eqn. (6–8).

$$k_{ET}(1 - R) = Rk_Q[O_2]^n \quad (6)$$

$$\left(\frac{1 - R}{R}\right) = \left(\frac{k_Q}{k_{ET}}\right)[O_2]^n \quad (7)$$

$$\log\left(\frac{1 - R}{R}\right) = \log\left(\frac{k_Q}{k_{ET}}\right) + n\log[O_2] \quad (8)$$

The spectral data depicted in Fig. 2—for the decay of $[Tb{\cdot}\mathbf{1}]^+$ as a function of oxygen in a sol–gel film prepared with an H_2O/Si ratio of 2—were treated according to eqn. (8). For each delay time studied between 0.06 and 0.71 ms, a separate plot of $\log[(1 - R)/R]$ *vs.* $\log[O_2]$ was made, which revealed straight lines with gradients of 0.48 (±0.02). By plotting the term $(1 - R)/R$ *versus* $[O_2]^{1/2}$, therefore, a linear variation was obtained and the sensitivity to oxygen quenching is given by the magnitude of the slope (Fig. 3). It is emphasised that such plots were used purely for calibration purposes to allow comparison between data sets.‡ In terms of a typical collisional quenching mechanism, the observed oxygen dependence does not seem to have a physical reality.

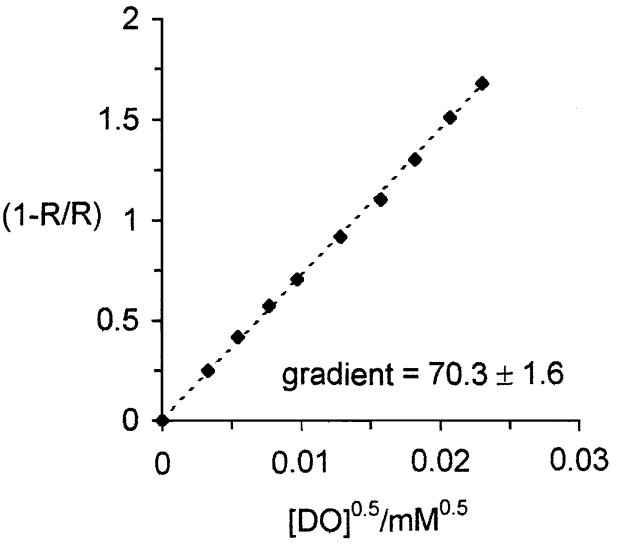

Fig. 3 Dependence of $[1 - (I_t/I_t^0)]/(I_t/I_t^0)$ on oxygen concentration for $[Tb{\cdot}\mathbf{1}]^+$ ($0.26 \leq t \leq 0.56$ ms; 295 K; $\lambda_{exc} = 330$ nm, $\lambda_{em} = 547$ nm).

The decay profiles for $[Tb{\cdot}\mathbf{1}]^+$ were examined on three occasions over a 5 month period, during which time the sensor was stored in air under ambient conditions. The average gradient of the response curve was 65 (±6) $mM^{-1/2}$, revealing good reproducibility and the absence of any serious film or complex degradation process. The modest sensitivity to oxygen is manifested in the Stern–Volmer plot (Fig. 4), with enhanced sensitivity below 0.1 mM O_2, *i.e.* below 3.2 ppm. An increased sensitivity to changes in $[O_2]$ was observed with sol–gel films of the tetraamide complex, $[Tb{\cdot}\mathbf{2}]^{4+}$. The intensity-based Stern–Volmer plot and 'linearised' decay data (Fig. 5) reveal an enhanced sensitivity at low $[O_2]$, and a mean gradient of 107 (±5) $mM^{-1/2}$ was established over a 5 month analysis period.

The improved sensitivity at low oxygen concentration of sol–gel films prepared with a H_2O/Si ratio of 2 has been observed previously.[30] Moreover, in films with a H_2O/Si ratio of 4, better sensitivity has been noted at higher O_2 concentra-

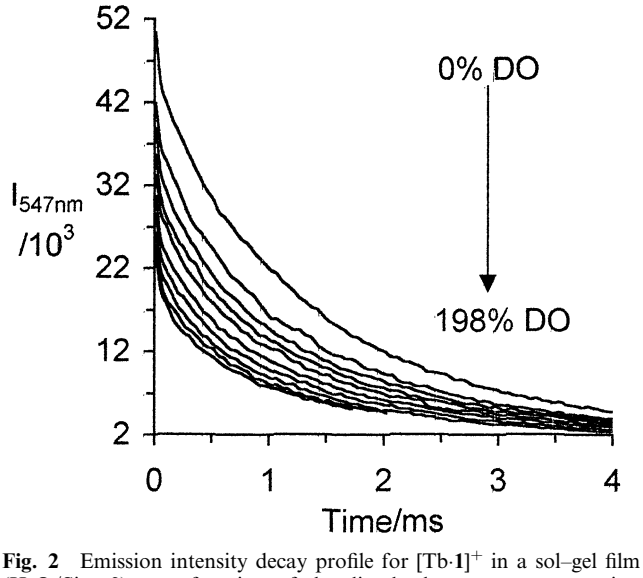

Fig. 2 Emission intensity decay profile for $[Tb{\cdot}\mathbf{1}]^+$ in a sol–gel film ($H_2O/Si = 2$) as a function of the dissolved oxygen concentration (295 K; $\lambda_{ex} = 330$ nm, delay increment 0.05 ms).

‡ Examples of data sets and the treatment thereof according to eqn. (8), at different delay times, are given in the ESI.

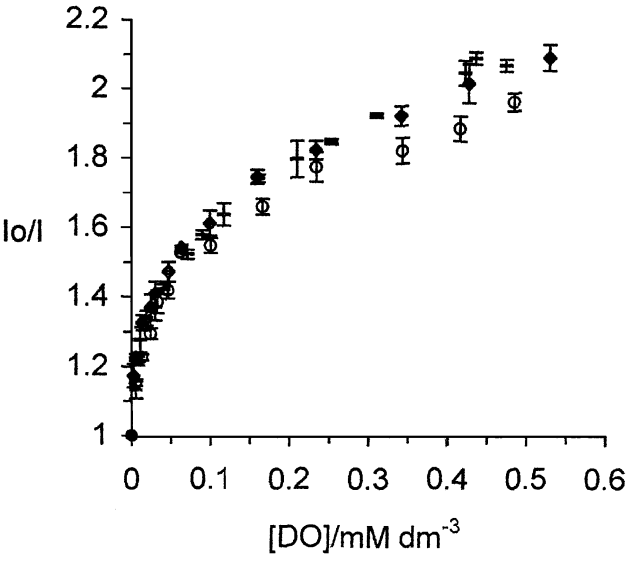

Fig. 4 Stern–Volmer plot for quenching of Tb emission in $[Tb{\cdot}\mathbf{1}]^+$ by O_2 over a 5 month period ($t = 1$, 2 and 5 months; 295 K; $\lambda_{ex} = 330$ nm, $\lambda_{em} = 547$ nm).

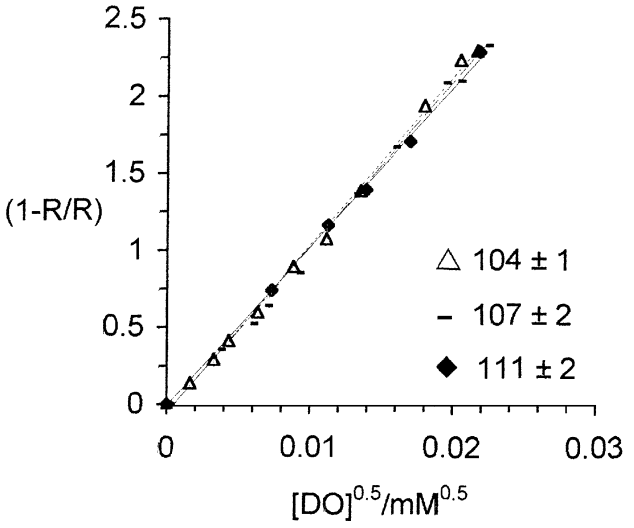

Fig. 5 Dependence of $[1-(I_t/I_t^0)/(I_t/I_t^0)]$ on oxygen concentration for $[Tb{\cdot}\mathbf{2}]^{4+}$ ($0.41 \leq t \leq 0.71$ ms; 295 K; $\lambda_{exc} = 330$ nm, $\lambda_{em} = 547$ nm), compared over a 5 month period [(——) $t = 1$, (△) $t = 3$, (◆) $t = 5$ months; mean gradient 107 $mM^{-1/2}$; $H_2O/Si = 2$].

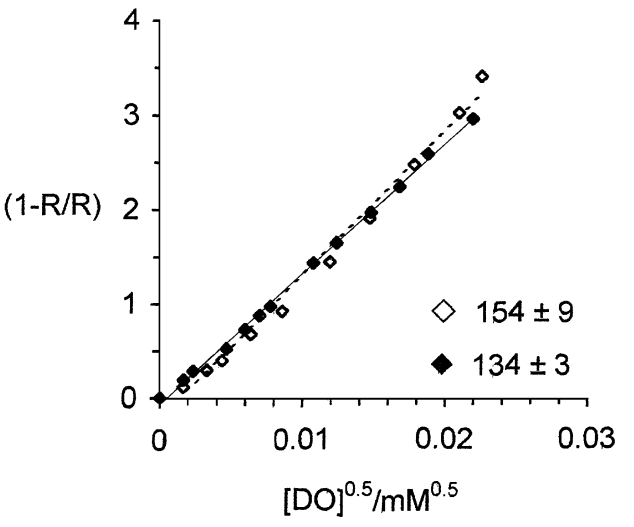

Fig. 7 Dependence of $[1-(I_t/I_t^0)/(I_t/I_t^0)]$ on oxygen concentration for $[Tb{\cdot}\mathbf{2}]^{4+}$ ($0.62 \leq t \leq 1.03$ ms; 295 K; $\lambda_{exc} = 330$ nm, $\lambda_{em} = 547$ nm) over a 3 month period [(◆) $t = 1$, (◇) $t = 3$ months; mean gradient 144 ± 12 $mM^{-1/2}$; $H_2O/Si = 4$].

tions, *i.e.* closer to the ambient level of *ca.* 0.27 mM. Accordingly, sol–gel films encapsulating $[Tb{\cdot}\mathbf{2}]^{4+}$ were prepared using a H_2O/Si ratio of 4. Such films are known to possess smaller average pore sizes,[25,26,30] leading to a reduction in the oxygen diffusion coefficient. A slightly more linear Stern–Volmer plot was obtained (Fig. 6), with an increased sensitivity to O_2 quenching, revealed most clearly in the calibration plot (Fig. 7). Hence, this sol–gel film exhibits the highest overall sensitivity (40% higher gradient than the film with $H_2O/Si = 2$) and is operative over the widest range of oxygen concentrations. Although certain species (*e.g.* Cl^- and Br^-) have been shown to quench the singlet excited state of the phenanthridinium chromophore used here,[17] this does not perturb the terbium emission decay profile. In control experiments, there was no change in the oxygen response in pre-determined solutions containing 10, 50 and 100 mM sodium chloride, measured at pH 3, 5 and 7. The sensor therefore is operative over the pH range 2–9 and in varying concentrations of common anions.

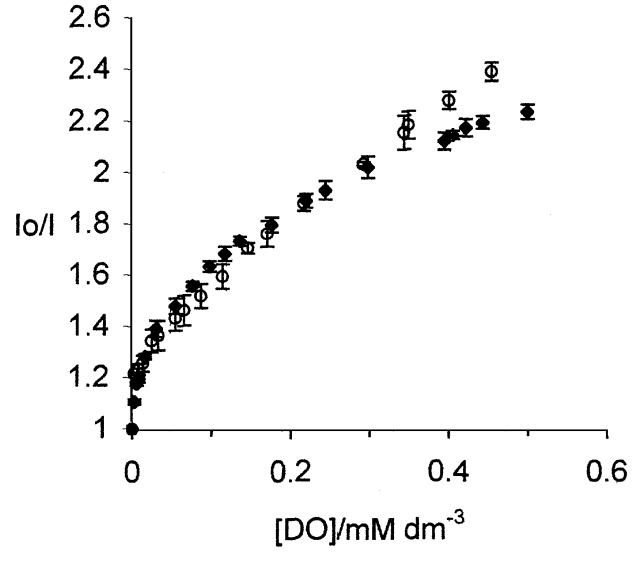

Fig. 6 Stern–Volmer plot for $[Tb{\cdot}\mathbf{2}]^{4+}$ quenching in the sol–gel matrix ($H_2O/Si = 4$) compared over a 3 month period [(○) $t = 1$, (◆) $t = 3$ months].

Conclusions

The high kinetic stability of the macrocyclic terbium complexes has allowed their physical entrapment in sol–gel thin films suitable for luminescence analysis. Notwithstanding the inherently complex decay kinetics associated with reversible sensitised terbium emission and the uncertainty introduced by site heterogeneity, a pragmatic treatment of emission decay curves has been established that allows comparison of analytical data for the same and different films. The sol–gel film prepared with a H_2O/Si ratio of 4, incorporating $[Tb{\cdot}\mathbf{2}]^{4+}$, exhibits good sensitivity to dissolved oxygen and represents the first example of lanthanide luminescence being used to signal changes in dissolved oxygen concentration in an operational sensor.

We thank the EPSRC for support and Dr Darren Noble for assistance with data linearisation.

References

1 I Klimant, F. Ruchrah, G. Liebsch, A. Stanelmayer and O. S. Wolfbeis, *Mikrochim. Acta*, 1999, **131**, 35.
2 M. R. Shahriari, J. Y. Ding, J. Tong and G. H. Sigel, *Proc. SPIE-Int. Soc. Opt. Eng.*, 1993, **2068**, 224.
3 J. N. Demas and B. A. DeGraff, *Anal. Chem.*, 1991, **63**, 829A.
4 H. Xu, J. W. Aylott, R. Kopelman, T. J. Miller and M. A. Philbert, *Anal. Chem.*, 2001, **73**, 4124.
5 W. Tan, R. Kopelman, S. C. R. Barker and M. T. Miller, *Anal. Chem.*, 1999, **71**, 606A.
6 K. P. McNamara and Z. Rosenzweig, *Anal. Chem.*, 1998, **70**, 4853.
7 H. W. Kroneis and H. J. Marsoner, *Sens. Actuators*, 1983, **4**, 587.
8 Y. Amao, K. Miyakawa and I. Okura, *J. Mater. Chem.*, 2000, **10**, 305.
9 A. Mills and A. Lepre, *Anal. Chem.*, 1997, **69**, 4653.
10 L. Sang-Kyung, B. S. Yong, P. Hyeon-Bong and H. P. Seon, *Chem. Lett.*, 2001, 310.
11 A. Mills *Platinum, Met. Rev.*, 1997, **41**, 115.
12 Y. Amao, K. Asai, I. Okura, H. Shinohara and H. Nishide, *Analyst*, 2000, **125**, 1911.
13 Y. Amao, K. Miyakawa and I. Okura, *Anal. Chim. Acta*, 2000, **421**, 167.
14 D. Parker, *Coord. Chem. Rev.*, 2000, **205**, 109.
15 F. J. Steemers, W. Verboom, D. N. Reinhoudt, E. B. van der Tol and J. W. Verhoeven, *J. Am. Chem. Soc.*, 1995, **107**, 9408.
16 A. Beeby, D. Parker and J. A. G. Williams, *J. Chem. Soc., Perkin Trans. 2*, 1996, 1565.

17 D. Parker, P. K. Senanayake and J. A. G. Williams, *J. Chem. Soc., Perkin Trans. 2*, 1998, 2129.
18 M. H. V. Werts, J. W. Verhoeven and J. W. Hofstraat, *J. Chem. Soc., Perkin Trans. 2*, 2000, 433.
19 M. H. V. Werts, R. H. Wondenberg, P. G. Emmerink, R. van Gassel, J. W. Hofstraat and J. W. Verhoeven, *Angew. Chem., Int. Ed.*, 2000, **39**, 4542.
20 A. Beeby, R. S. Dickins, S. FitzGerald, L. J. Govenlock, C. L. Maupin, D. Parker, J. P. Riehl, G. Siligardi and J. A. G. Williams, *Chem. Commun.*, 2000, 1183.
21 Y. Amao, I. Okura and T. Miyashita, *Chem. Lett.*, 2000, 934.
22 Y. Amao, I. Okura and T. Miyashita, *Bull. Chem. Soc. Jpn.*, 2000, **73**, 2663.
23 Y. Amao, I. Okura and T. Miyashita, *Chem. Lett.*, 2000, 1286.
24 D. R. Uhlmann, G. Teowee and J. Boulton, *J. Sol-Gel Sci. Technol.*, 1997, **8**, 1083.
25 C. M. McDonagh, A. M. Shields, A. K. McEvoy, B. D. MacCraith and J. F. Gouin, *J. Sol-Gel Sci. Technol.*, 1998, **13**, 207.
26 C. McDonagh, C. Kolle, A. K. McEvoy, D. L. Dowing, A. A. Cafolla, S. J. Cullen and B. D. MacCraith, *Sens. Actuators, B*, 2001, **74**, 124.
27 G. Bobba, R. S. Dickins, S. D. Kean, C. E. Mathieu, D. Parker, R. D. Peacock, G. Siligardi, M. J. Smith, J. A. G. Williams and C. F. G. C. Geraldes, *J. Chem. Soc., Perkin Trans. 2*, 2001, 1729.
28 I. M. Clarkson, A. Beeby, J. I. Bruce, L. J. Govenlock, M. P. Lowe, C. E. Mathieu, D. Parker and P. K. Senanayake, *New J. Chem.*, 2000, **24**, 377.
29 S. Blair, R. Kataky, M. P. Lowe, C. E. Mathieu, D. Parker and P. K. Senanayake, *Inorg. Chem.*, 2001, **40**, 5860.
30 C. McDonagh, B. D. MacCraith and A. K. McEvoy, *Anal. Chem.*, 1998, **70**, 45.
31 K. Kimura, S. Yajima, H. Takase and M. Yokoyama, *Anal. Chem.*, 2001, **73**, 1605.
32 L. Sacksteder, J. N. Demas and B. A. DeGraff, *Anal. Chem.*, 1993, **65**, 3480.
33 J. N. Demas, *Excited State Lifetime Measurements*, Academic Press, New York, 1983, pp. 59–66.